J Therm Anal Calorim (2010) 102:203–210
DOI 10.1007/s10973-010-0685-0

Thermal and structural characterization of two polymorphs of Atovaquone and of its chloro derivative

Luciana Malpezzi · Claudio Fuganti · Elisabetta Maccaroni · Norberto Masciocchi · Antonio Nardi

Received: 21 May 2009 / Accepted: 13 January 2010 / Published online: 4 February 2010

Abstract Atovaquone, 2-[4-(4-chlorophenyl)cyclohexyl]-3-hydroxy-1,4-naphthoquinone, is an antimicrobial medicament used to treat or prevent *pneumocystis carinii pneumonia*, *toxoplasmosis* and *malaria.* Two polymorphs of Atovaquone (crystal phases I and III) were isolated and their crystal and molecular structures were determined by single crystal X-ray analysis. In both crystal phases, strong hydrogen bond interactions link adjacent molecules in centrosymmetric dimers. The existence of the different polymorphs is determined by the different orientation of the dimers in the crystal packing. In addition, a crystalline phase of the 2-chloro substituted derivative, which is not stabilized by intermolecular H-bond interactions, was also studied, and compared with those of the pristine (hydroxylic) species. DSC measurements and thermodiffractometry analyses on polycrystalline batches witnessed the 100% purity of the isolated materials and disclosed the crystal-to-crystal interconversion of phase I to phase III upon heating at 210 °C.

Keywords Atovaquone · Polymorphism · Crystal and molecular structure · Thermodiffractometry · Thermal analysis

L. Malpezzi · C. Fuganti
Dipartimento di Chimica, Politecnico di Milano, via Mancinelli 7, 20131 Milan, Italy

E. Maccaroni (✉) · N. Masciocchi
Dipartimento di Scienze Chimiche e Ambientali, Università dell'Insubria, via Valleggio 11, 22100 Como, Italy
e-mail: emaccaroni@gmail.com

A. Nardi
Labochim, Via B. Cellini 20, 20090 Segrate, Italy

Introduction

The existence of different crystalline and/or amorphous phases for a drug prepared, processed or marketed as a solid material is raising an increasing interest in most pharmaceutical companies; indeed, different polymorphic forms, possessing distinct molecular shapes, arrangements, and interatomic contacts, typically exhibit different physical properties: dissolution rate, solubility, stability, bioavailability, etc. [1–3], severely affecting, among other features, drug processibility, pharmaceutical formulation and, above all, therapeutic efficiency. Therefore, nowadays it is a common practice in the pharmaceutical field, to deeply investigate the polymorphic behavior of a drug, allowing a deep control on the way molecules crystallize, aiming at producing materials with specific and reproducible properties and at optimizing their production processes and also their storage conditions. Accordingly, the complete characterization of the solid-state properties of the active ingredients, of the excipients as well as of their mixtures is a mandatory step, which cannot be neglected during drug development [4]. Following recent studies in the thermal and structural characterization of commonly marketed drugs, to mention a few: Theophylline, Norfloxacin, Acitretin, Linezolid, Azelastine, and Sibutramine [5–10], we have focused our attention to the crystal chemistry of Atovaquone, which has been described as being polymorphic in the patent literature [11], but, to the best of our knowledge, has not been structurally investigated.

Atovaquone, 2-[4-(4-chlorophenyl)cyclohexyl]-3-hydroxy-1,4-naphthoquinone (see Scheme 1), is an antimicrobial medicament used to treat or prevent *pneumocystis carinii pneumonia*, *toxoplasmosis*, and *malaria* [12]. Pioneering studies on antimalarials [13] during World War II allowed to design the new class of hydroxynaphthoquinone

derivatives. Further optimization of this class of drugs during the 1980s led to the development of Atovaquone, a hydroxynaphthoquinone with a cyclohexyl-chlorophenyl group in 2 position of the quinone [14]. This molecule was found to possess a broad anti-parasitic spectrum and to enhance good pharmacokinetic properties [15]. In recent years, Atovaquone is often combined with another anti-malarial, *proguanil*, which works in a synergic manner against drug-resistant parasites, such as *Plasmodium falciparum* [16]. In this combination, it was approved for use in the antimalaria protocols already in the mid-1990s in Europe and only later, in 2000, by FDA. Accordingly, Atovaquone-proguanil drugs are now strongly recommended for travelers visiting all malaria-endemic countries.

Solid Atovaquone is a yellow crystalline material, practically insoluble in water. Only very recently, the WO 2006/008752-A1 application *claimed* the *discovery* of three different crystalline forms, which have been characterized by thermal analysis (DSC) and X-ray powder diffraction.

Polymorph I and polymorph III (hereafter named Ato-I and Ato-III, respectively) were obtained in our laboratory, upon crystallization from suitable solvents under appropriate conditions (described below), in form of crystals suitable for conventional single crystal X-ray analysis. On the contrary, any attempt to obtain polymorph II, as characterized by XRPD on the WO 2006/008752-A1 application, following the examples described therein, failed. Consequently, this study describes the molecular and crystalline structures of two polymorphs of Atovaquone, Ato-I and Ato-III, aiming at comprehending the most significant structural differences between the two crystalline modifications, and correlating them with the thermal behavior, as studied by TG and DSC analyses. In order to complete our structural study, we also investigated the structure of a halo-substituted derivative, 2-[4-(4-chlorophenyl)-cyclohexyl]-3-chloro-1,4-naphthoquinone (hereafter named Ato-Cl), which is a precursor in the preparation of atovaquone and possesses similar steric features, but significantly different electronic properties (particularly of the acid–base type).

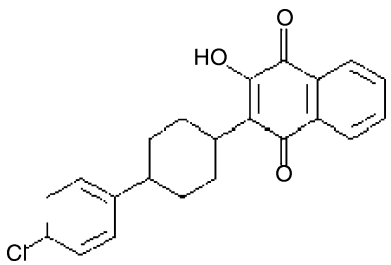

Scheme 1 Schematic drawing of the Atovaquone molecule

Experimental

Materials

Chemically pure atovaquone, in solid form, was provided by Labochim S.p.A, Milano, Italy. It was recrystallized (as described below) from hot *n*-heptane or acetonitrile affording form I and form III, respectively. The two forms can be easily and rapidly distinguished, since crystals of form I are yellow, while those of form III show a definite orange hue.

Isolation of form I, Ato-I 0.49 g of crude atovaquone was dissolved in 10 ml of refluxing dichloromethane at 40 °C. After cooling, 10 ml of *n*-heptane was added dropwise to this solution. The mixture was refluxed for 4 h with stirring and then slowly cooled. A yellow solid was obtained and then filtered and dried under vacuum. Among very small crystals, a suitable specimen for conventional X-ray analysis was found.

Isolation of form III, Ato-III 1.0 g of crude atovaquone was dissolved in 15 ml of acetonitrile at 40 °C. Acetonitrile was distilled out to concentrate the solution until turbidity. A few drops of acetonitrile were added and the clear solution was allowed to cool to room temperature. Orange crystals, suitable for X-ray analysis, were grown by slow evaporation of the solvent.

Isolation of Ato-Cl, 1.0 g of the crude product, prepared in our laboratory following the procedure reported in the patent literature [17], was dissolved in 10 ml of dioxane and a few drops of THF. THF was removed from the solution by distillation and the remaining solution was allowed to cool to room temperature. Yellow crystals, suitable for X-ray analysis, were grown by slow evaporation of the solvent.

Single crystal X-ray diffraction

Single crystal X-ray diffraction data (SCXRD) were collected on a Siemens P4 diffractometer with graphite monochromated Cu-Kα radiation ($\lambda = 1.5418$Å), for Ato-III and Ato-Cl, and on a Enraf–Nonius CAD4 diffractometer with graphite monochromated Mo-Kα radiation ($\lambda = 0.71073$ Å) for Ato-I. Accurate unit cell parameters were determined by least-squares analysis of angular data of 25 reflections for Ato-I (in the range $9° \leq 2\theta \leq 12°$), 44 reflections for Ato-III (in the range $9.8° \leq 2\theta \leq 72°$) and 58 reflections for Ato-Cl (in the range $14.4° \leq 2\theta \leq 36.0°$).

Data collection and data reduction strategy followed standard procedures implemented in the diffractometers software. The structures were solved by direct methods using SIR97 program [18] and refined on F^2 by full-matrix least-squares procedure, SHELXL-97 [19], with anisotropic temperature factors for all non-H atoms. In each

structure, H atoms (apart from the hydroxylic ones which were freely refined with individual isotropic temperature factors) were placed in geometrically calculated positions and refined by a riding model. Crystal data and refinement details are summarized in Table 1. CCDC No. 7114426, 714427 and 714428 for Ato-I, Ato-III, and Ato-Cl, in the order.

X-ray powder diffraction

The X-ray powder diffraction (XRPD) patterns of Ato-I, Ato-III and Ato-Cl were collected at room temperature on an Ital-Structure θ/θ automated diffractometer, under the following conditions: Ni-filtered CuKα radiation ($\lambda =$ 1.5418 Å); range $3° \leq 2\theta \leq 40°$ (no significant peaks could be observed at higher diffraction angles); $\Delta 2\theta = 0.04°$; $t = 2$ s step^{-1}. The XRPD patterns were also calculated from the atomic coordinates determined by single crystal analysis, using Mercury [20]. On comparing the experimental and calculated traces, some unavoidable variations in the corresponding peak intensities (but not location) were observed, and ascribed to preferred orientation effects, a phenomenon frequently observed during data collection of morphologically anisotropic organic compounds. However, for each compound the experimental and calculated XRPD patterns are in complete agreement in the sequence of the diffracted peaks positions and appear unambiguously to describe the same crystalline phase.

Non-ambient diffraction data (TXRPD) were collected in the 5–35° 2θ range, sampling at 0.02°, on a θ:θ vertical scan Bruker AXS D8 Advance diffractometer, equipped with a linear Lynxeye position sensitive detector, set at 300 mm from the sample (Ni-filtered Cu-K$\alpha_{1,2}$ radiation, $\lambda = 1.5418$ Å) and using a custom made heating chamber which allows to raise the temperature, in air, in a controlled manner, up to 600 °C.

Thermogravimetric analysis and differential scanning calorimetry

TG and DSC measurements were simultaneously performed on a Netzsch STA 409 PC LUXX apparatus at scanning rate of 10 °C min^{-1}, in the 40–450 °C temperature range. The sensor and the samples were maintained under a nitrogen purge during the whole experiment. Transition temperatures in the DSC traces were determined by the onset method, i.e., taking the temperature value

Table 1 Crystal data and data collection parameters for the three species Ato-I, Ato-III and Ato-Cl

	Ato-I	Ato-III	Ato-Cl
Formula	$C_{22}H_{19}ClO_3$	$C_{22}H_{19}ClO_3$	$C_{22}H_{18}Cl_2O_2$
Molecular weight/g mol^{-1}	366.82	366.82	385.26
Temperature/K	293	293	293
Crystal system	Monoclinic	Monoclinic	Monoclinic
Space group	$P2_1/n$	$P2_1/c$	$P2_1/n$
Color	Yellow	Yellow	Orange
Cell parameters/Å or °	$a = 5.918(2)$	$a = 12.535(1)$	$a = 10.343(1)$
	$b = 18.351(4)$	$b = 5.267(1)$	$b = 7.056(1)$
	$c = 16.629(3)$	$c = 27.809(4)$	$c = 25.070(2)$
	$\alpha = 90$	$\alpha = 90$	$\alpha = 90$
	$\beta = 97.25(1)$	$\beta = 92.59(1)$	$\beta = 99.80(1)$
	$\gamma = 90$	$\gamma = 90$	$\gamma = 90$
V/Å^3	1791.5(1)	1834.1(5)	1802.9(3)
Z	4	4	4
ρ calc/g cm^{-3}	1.353	1.328	1.419
F(000)	768	768	800
Radiation	Mo-Kα	Cu-Kα	Cu-Kα
θ min–max	3.3–25.3	3.2–65	4.4–65
Total reflections	3,136	4,255	3,894
Independent reflections/parameters	3136/258	2985/258	2813/260
R_{int}	0.058	0.070	0.059
Observed data [$I > 2\sigma(I)$] refinement	1582	2120	1543
R, wR_2	0.053, 0.104	0.062, 0.155	0.065, 0.139

E.s.d.'s in parentheses

measured at the crossing point between the baseline and the tangent segment taken at the lower inflection point of the endothermic peaks.

Results and discussion

It is well known that each crystalline modification of a product is associated with a diffraction pattern that can be used to identify, e.g., the pertinent polymorphic form during the successive steps of the drug development, process and storage. Accordingly, the X-ray powder diffraction patterns of the three compounds, drawn in Fig. 1, show very distinct features, favouring a rapid and easy assessment of the nature of the powders, as well as allowing quantification of the different species, by conventional or full pattern quantitative analysis [21]; therefore, the joint use of suitable equipment and data analysis procedures constitute valuable tools in the pharmaceutical chemist's hands, which greatly benefit from the knowledge of the accurate structure models, simplifying the computational

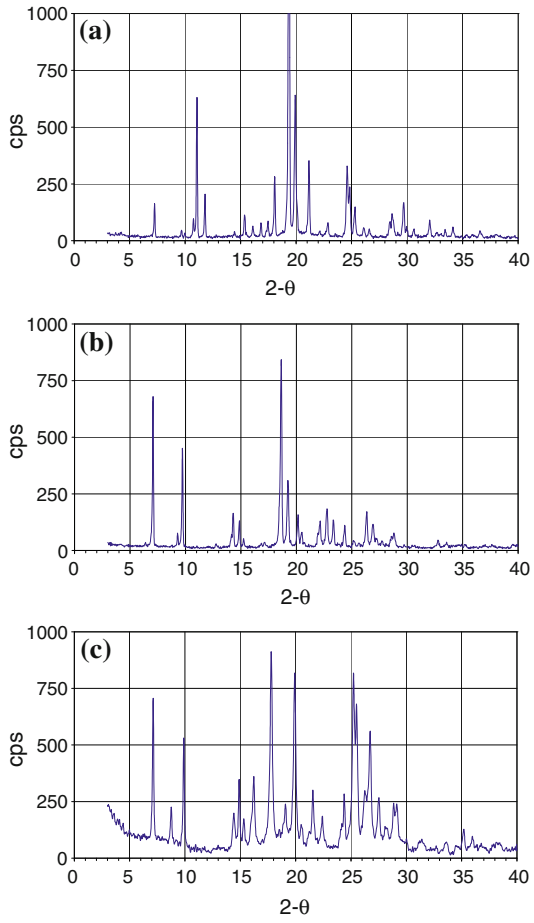

Fig. 1 X-ray powder diffraction traces for Ato-I (**a**), Ato-III (**b**), and Ato-Cl (**c**)

Table 2 Main diffraction peaks for the three species Ato-I, Ato-III, and Ato-Cl, reported as *d*/hkl/*I* triplets

Ato-I			Ato-III			Ato-Cl		
d	hkl	I	d	hkl	I	d	hkl	I
12.290	011	4	12.522	100	29	12.352	002	9
8.261	020	8	9.098	102	33	10.044	−101	9
8.034	021	10	6.193	−104	11	8.903	101	18
7.536	012	12	5.960	104	13	6.127	012	17
5.775	−101	10	4.759	−204	70	5.931	102	11
5.510	−111	6	4.608	−11	100	5.774	−111	10
5.276	013	8	4.408	−106	15	5.530	111	10
5.121	111	5	4.331	−113	26	5.459	−112	30
4.922	032	9	4.012	−114	42	4.975	−113	100
4.597	040	68	3.901	−212	70	4.647	014	18
4.463	−122	100	3.806	−206	18	4.449	−114	88
4.203	−131	46	3.645	206	8	4.091	−212	12
3.895	−123	15	3.531	−214	11	3.955	−115	19
3.622	140	55	3.380	−116	68	3.638	204	16
3.597	−141	13	3.309	−215	43	3.528	020	23
3.140	−143	13	3.271	310	15	3.526	−107	26
3.118	150	15	3.210	−312	13	3.508	−206	15
			3.119	−313	16	3.493	021	85
			3.099	−117	19	3.392	022	49
						3.243	120	74
						3.063	−121	13

Intensities are normalized to the highest peak, taken as 100; *d*-spacings in Å. The intensities of the reported reflections were calculated from the atomic coordinates determined by X-ray single crystal analysis, in order to have values free from preferred orientation effects

analysis in both qualitative and quantitative aspects. However, phase identification by means of XRPD data often relies on a simple *d*/*I* list only, which is nearly independent on the degree of crystallinity of the sample and on the experimental conditions (radiation, optics, etc.) locally employed. For this reason, Table 2 contains the pertinent values which can be safely used in recognizing and/or addressing a specific crystalline phase.

Our complete single-crystal structural analysis, the results of which are briefly reported in Table 3 (containing the relevant geometric parameters describing the molecular shape and conformations), shows that the three molecules, in the different crystal phases, possess similar bond distances and angles. For the sake of simplicity, only one ORTEP drawing is shown here in Fig. 2, that of the Ato-I polymorph. The six-membered aliphatic rings are found in chair conformation in all the three crystal phases, with a *trans*-equatorial location of the aromatic residues. The most significant differences among these moieties lie in the mutual disposition of the phenyl and naphthoquinone rings, addressed by dihedral angles of 11.7(3)°, 5.1(3)°, and

Table 3 Selected bond distances (Å) and angles (°) for the three species Ato-I, Ato-III, and Ato-Cl

	Ato-I	Ato-III	Ato-Cl
C2–O1	1.221(4)	1.221(4)	1.208(5)
C9–O2	1.223(4)	1.218(4)	1.208(5)
C10–O3,Cl2	1.350(4)	1.346(4)	1.719(5)
C2–C1···C17–C18	171.7(3)	177.3(3)	173.1(3)
C10–C1···C17–C18	−14.60(4)	−3.5(4)	−8.3(5)
Cl1···C6	15.34(6)	15.21(5)	15.20(6)
C2–C1–C11–C16	−75.20(4)	−63.8(4)	−74.0(6)
C13–C14–C17–C18	63.8(4)	63.8(4)	63.6(7)

E.s.d's in parentheses

14.7(3)° for Ato-I, Ato-III, and Ato-Cl, in the sequence. A view of the relative orientation of the phenyl and naphthoquinone ring Ato-I (a), Ato-III (b), and Ato-Cl (c), is shown in Fig. 3.

These small differences may not per se explain the variability of the crystal packing. Indeed, the presence of different molecular arrangement in the solid is mainly due, in these cases, to the different supramolecular contacts, mostly of the hydrogen-bond type.

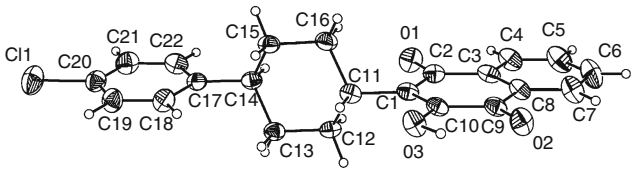

Fig. 2 Molecular structure of Ato-III, showing the atom-numbering scheme adopted for both polymorphs. The same atom-labeling was also adopted for Ato-Cl, with the obvious substitution of Cl2 for O3

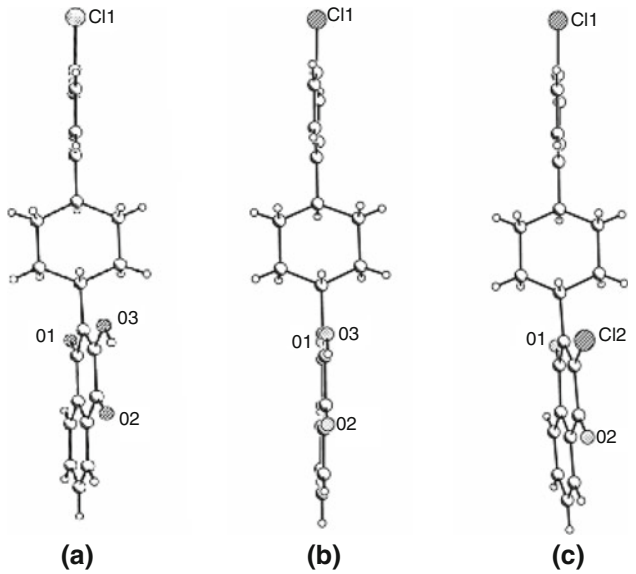

Fig. 3 A view of the relative orientations of the phenyl and naphthoquinone ring in Ato-I (**a**), Ato-III (**b**) and Ato-Cl (**c**)

As shown in Fig. 4a, in Ato-I the molecules form dimers *via* two O3–H···O2 hydrogen bonds across crystallographic centres of symmetry. These are the most significant (stabilizing) interactions, while no markedly short intermolecular contacts occur between the dimers. Along *b* direction the dimers are stacked in antiparallel orientation forming a zig-zag motif (Table 4).

Also in Ato-III, molecules are arranged in centrosymmeric dimers through the same O3–H···O2 hydrogen bond; however, other weaker contacts are present (see the C13–H···O1 link in Fig. 4b), allowing the propagation of a two dimensional sheet in the *bc* plane. All the dimers, inside the same sheets or in adjacent sheets, have the same orientation. Therefore, given also the very similar conformations of atovaquone moieties in the Ato-I and Ato-III polymorphs, it is the difference in the reciprocal orientation of the dimers which explains the existence of two polymorphs of atovaquone. These observations may also suggest that crystallization of atovaquone in non-equilibrium conditions may lead to a polytypic material, where the sequence of the molecules is aperiodic and highly defective. If ever achieved, this material may exhibit slightly different properties, such as an enhanced solubility.

At variance, the crystal packing of Ato-Cl is governed by only C21–H···Cl2 short interactions that link the molecules into antiparallel chain running parallel to *ac* plane (see Fig. 4c). In this crystal phase there are no specific interactions between adjacent chains; accordingly, a lower

Table 4 List of significant H-bonding interactions (Å, °) for Ato-I, Ato-III, and Ato-Cl

D–H…A	d(D–H)	d(H···A)	d(D···A)	<(DHA)
Ato-I[a]				
O3–H3···O2#1	0.89(4)	2.00(4)	2.782(4)	146(4)
O3–H3···O2	0.89(4)	2.21(4)	2.662(4)	111(3)
Ato-III[b]				
O3–H3O···O2#1	0.86(4)	2.05(5)	2.809(3)	146(4)
C13–H13B···O1#2	0.97	2.55	3.496(4)	165.9
O3–H3O···O2	0.86(4)	2.15(4)	2.643(3)	116(4)
C16–H16B···O1	0.97	2.50	3.110(4)	120.6
Ato-Cl[c]				
C11–H11···Cl2	1.01(4)	2.51(4)	3.081(5)	116(3)
C12–H12B···O1	0.97	2.34	2.978(6)	122.4
C7–H7···O2	0.93	2.56	2.823(7)	96.9
C21–H21···Cl2#1	0.93	2.86	3.744(5)	160.1

Symmetry transformations used to generate equivalent atoms:

[a] #1 $-x-1, -y+2, -z$

[b] #1 $-x+1, -y-1, -z+1$; #2 $-x+1, y-1/2, -z+1/2$

[c] #1 $x-1/2, -y+1/2, z-1/2$

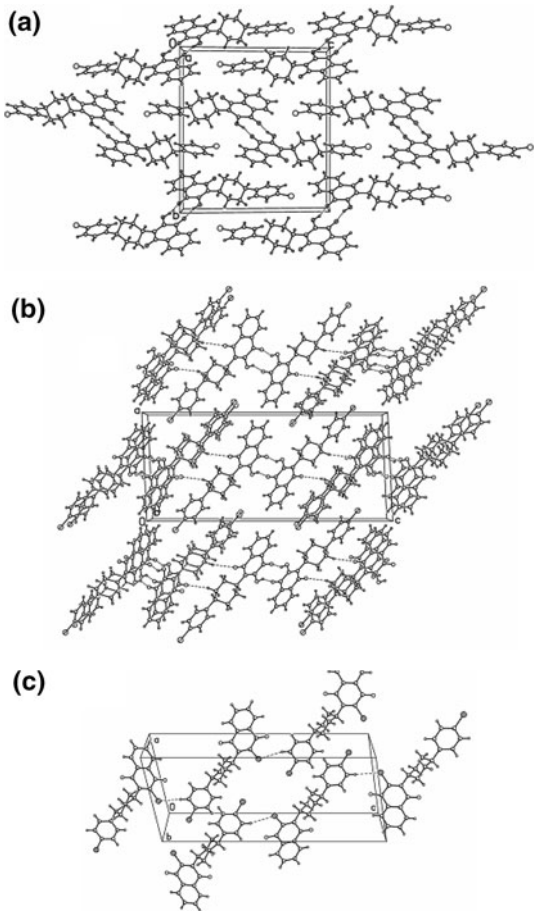

Fig. 4 Schematic drawing of the crystal packing of the three species: Ato-I (**a**) (formation of dimers *via* O–H···O hydrogen bonds); Ato-III (**b**) (formation of two-dimensional sheets in the *ac* plane *via* a C–H···O hydrogen bonds joining the dimers), and Ato-Cl (**c**) (formation of chains running parallel to the ac plane via C–H···Cl short interactions)

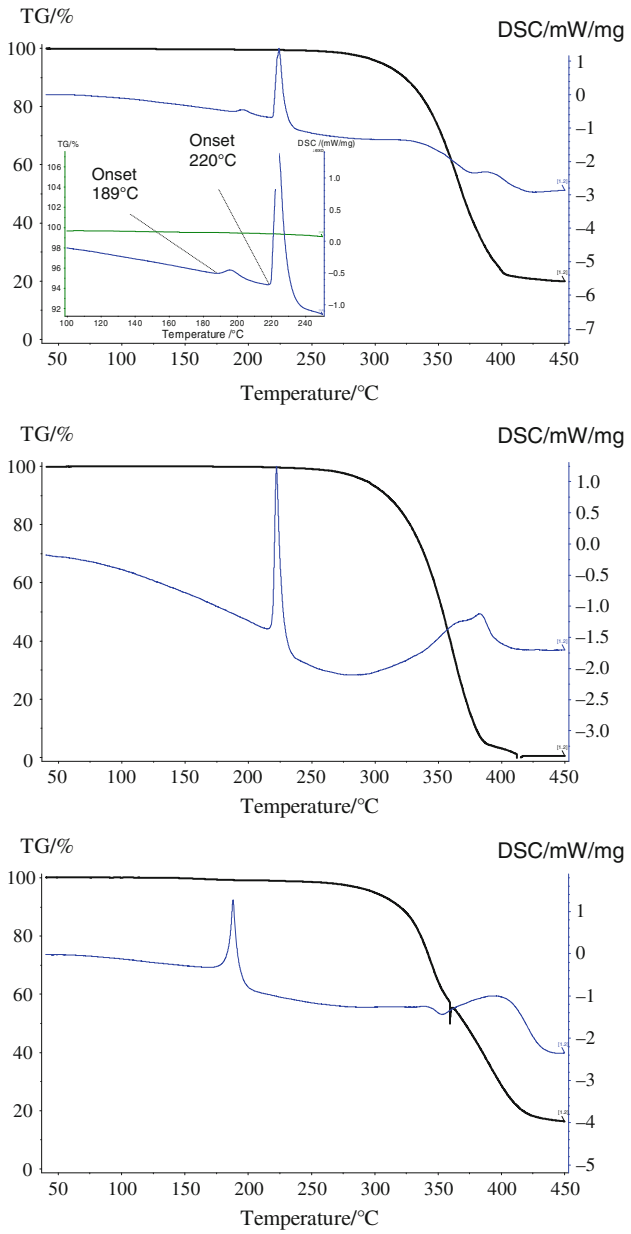

Fig. 5 TG and DSC traces of Ato-I, Ato-III, and Ato-Cl (*top to bottom*). The *inset* in the DSC trace of Ato-I shows highlights the solid–solid phase transition at a magnified scale

melting point, as derived from the DSC traces discussed below, is observed.

Solid-state interconversions of atovaquone forms I and III

The DSC traces of Ato-I, Ato-III, and Ato-Cl are depicted in Fig. 5. Ato-III and Ato-Cl show a single endothermic peak corresponding to a melting process, occurring at 220 °C ($\Delta H = 35$ kJ mol^{-1}) and 184 °C ($\Delta H = 35$ kJ mol^{-1}), respectively. Ato-I shows an additional small endothermic process 189 °C ($\Delta H = 2.5$ kJ mol^{-1}), immediately followed by a melting peak coincident with that of Ato-III. The first thermal event can be safely attributed to the solid state transformation of form I into form III (as confirmed by thermodiffractometric measurements).

Actually, Ato-III has the lowest crystal packing density (1.328 vs. 1.353 g cm^{-3} for form I) and according to the "density rule" it should be the metastable form [22]. It is, however, well known [23, 24] that this rule is often broken if significantly different hydrogen-bond interactions are present in the crystals, as in the present case: Ato-III shows, beyond conventional O–H···O hydrogen-bond interactions, additional weak contacts [C13–H···O2 and C16–H···O1], which are absent in Ato-I.

Our TG analysis performed on Ato-III and Ato-Cl samples indicated no mass losses before melting; this is also true for the Ato-I material, and, significantly, confirms

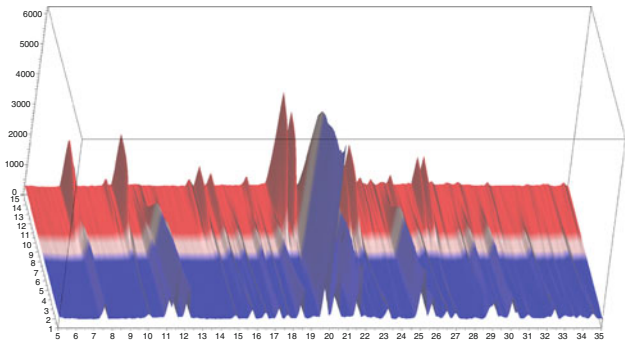

Fig. 6 Thermodiffractometric plot for Ato-I transforming into Ato-III (*bottom to top*). The *lowest* and *middle* portion of the graph show data measured on heating from 30 °C to 210 °C, while the *upper* section was measured keeping the sample under isothermal conditions, 210 °C, for about 30 min

the crystal-to-crystal (not desolvation) nature of the small endothermic event occurring near 190 °C.

Thermodiffractometry

The interpretation above derived by DSC data was confirmed by collecting XRPD patterns at different temperatures directly in the diffractometer chamber. Progressive heating up to 210 °C showed that Ato-I can be completely transformed into Ato-III. The small discrepancy between the XRPD and DSC transformation temperatures here observed are likely related to temperature gradients for a bulkier sample (in the XRPD experiment) than that used in the DSC oven.

The Ato-I → Ato-III phase transformation does not occur through the formation of a detectable amorphous phase. After the phase transition, the sample was further heated to about 250 °C, inducing evident melting, and cooled back to ambient temperature within minutes: crystallization to Ato-III form was observed, with no detectable traces of form I. In the used conditions, it appears that the crystal-to-crystal phase transition is irreversible, leading to the formation of the thermodynamically stable polymorph Ato-III. Figure 6 shows the complete 2-D thermodiffractogram, highlighting the solid-state transformation occurring near 200 °C.

Conclusions

In this article, we have reported the thermal and structural characterization of two polymorphs of Atovaquone (crystal phases I and III). In both crystal phases, strong hydrogen bonds link adjacent molecules in centrosymmetric dimers, whose different orientation in the crystal packing causes the existence of the two polymorphic forms, which, therefore, are not of the conformational type. TG and DSC measurements on polycrystalline batches demonstrated the 100% purity of the isolated materials and disclosed the crystal-to-crystal interconversion of phase I to phase III promoted by heating, eventually followed by in situ thermodiffractometric methods. Thus, a combination of thermal and structural analyses of different types (TG, DSC, SCXRD, XRPD, and TXRPD) led to a coherent picture of the crystal chemistry of Atovaquone, further substantiated by ancillary thermal and structural studies of the chloro derivative, which cannot form the highly stabilizing network of hydrogen-bond interactions.

References

1. Bernstein J. Polymorphism of pharmaceuticals. In: Polymorphism in molecular crystal. Oxford Science Publications, Oxford; 2002, pp 240–256.
2. Brittain HG. Polimorphism in pharmaceutical Solids. New York: Marcel Dekker Inc.; 1999.
3. Hilfiker RH. Polymorphism in the pharmaceutical industries. Weinheim, Germany: Wiley-VCH Verlag GmbH & Co; 2006.
4. Giron D, Mutz M, Garnier S. Solid-state of pharmaceutical compounds. J Therm Anal Calorim. 2004;77:709–47. (and references therein).
5. Szterner P, Legendre B, Sghaier M. Thermodynamics properties of polymorphic forms of theophylline. Part I: DSC, TG, X-ray study. J Therm Anal Calorim. 2009. doi:10.1007/s10973-009-0186-1.
6. Barbas R, Prohens R, Puigjaner C. A new polymorph of norfloxacin. Complete characterization and relative stability of its trimorphic system. J Therm Anal Calorim. 2007;89:687–92.
7. Malpezzi L, Magnone GA, Masciocchi N, Sironi A. Single crystal and powder diffraction characterization of three polymorphic forms of Acitretin. J Pharm Sci. 2005;94:1067–78.
8. Maccaroni E, Alberti A, Malpezzi L, Masciocchi N, Vladiskovic C. Polymorphism of linezolid: a combined single-crystal, powder diffraction and NMR study. Int J Pharm. 2008;351:144–51.
9. Maccaroni E, Alberti A, Malpezzi L, Mazzetti G, Vladiskovic C, Masciocchi N. Azelastine Hydrochloride: a power diffraction and ^{13}C CPMAS NMR study of its anhydrous and solvated forms. Cryst Growth Des. 2009;9:517–24.
10. Maccaroni E, Alberti A, Malpezzi L, Masciocchi N, Pellegatta C. Crystal chemistry of Sibutramine: thermal, diffractometric and spectroscopic characterization. J Pharm Sci. 2008;97:5229–39.
11. Tarur VR. Novel Polymorphs of atovaquone and process of preparation thereof. US 2006/0241311 A1; 2006.
12. Hughes WT, Gray V, Gutteridge WE, Latter VS, Pudney M. Efficacy of a hydroxynaphthoquinone, 566C80, in experimental *Pneumocystis carinii* pneumonitis. Antimicrob Agents Chemother. 1990;34:225–8.
13. Fieser LF, Berliner E, Bondhus FJ, Chang FC, Dauben WG, Ettlinger MG, et al. Naphthoquinone antimalarials I. J Am Chem Soc. 1948;70:3151–5.
14. Hudson AT. Atovaquone-a novel broad-spectrum anti-infective drug. Parasitol Today. 1993;9:66–8.
15. Watkins ER, Meshnick SR. Drugs for malaria. Sem Pediatr Infect Dis. 2000;11:202–12.
16. Kessl JJ, Meshnick SR, Trumpower BL. Modelling the molecular basis of Atovaquone resistance in parasites and pathogenic fungi. Trends Parasitol. 2007;23:494–501.

17. Latter VS, Gutteridge WE. Medicaments. US 4981874; 1991.
18. Altomare A, Burla MC, Cavalli M, Cascarano GL, Giacovazzo C, Gagliardi A, et al. SIR97: a new tool for crystal structure determination and refinement. J Appl Cryst. 1999;32:115–9.
19. Sheldrick GM. SHELXL-97. Program for the refinement of crystal structures. Germany: University of Göttingen; 1997.
20. Macrae CF, Edgington PR, McCabe P, Pidcock E, Shields GP, Taylor R, et al. Mercury: visualisation and analysis of crystal structures. J Appl Cryst. 2006;39:453–7.
21. Jenkins R, Snyder RL. Introduction to X-ray powder diffractometry. New York: Wiley; 1996.
22. Burger A, Ramberger A. On the polymorphism of pharmaceuticals and other molecular crystal. I. Theory and thermodynamics rules. Mikrochim Acta. 1979;2:259–71.
23. Burger A, Ramberger A. On the polymorphism of pharmaceuticals and other molecular crystal. II. Applicability and thermodynamics rules. Mikrochim Acta. 1979;2:273–316.
24. Chen X, Morris KR, Griesser UJ, Byrn SR, Stowell JG. Reactivity differences of Indomethacin solid forms with ammonia gas. J Am Chem Soc. 2002;124:15012–9.